

ORIGINAL RESEARCH

# Exploring Associations Between Cardiac Structure and Retinal Vascular Geometry

Lihua Huang, MBBS; Izzuddin M. Aris, PhD; Louis L. Y. Teo, MBBS; Tien Yin Wong, MD, PhD; Wei-Qing Chen, MD, PhD; Angela S. Koh, MBBS, MPH\*; Ling-Jun Li , MD, PhD\*

**BACKGROUND:** Retinal arteriolar narrowing and venular widening has been widely suggested to be associated with subclinical changes in cardiac structure. The novel retinal vascular geometric indices might reflect more comprehensive information on microvasculature other than vascular caliber alone. However, the association between suboptimal retinal vascular geometry and cardiac structural alteration has not been studied.

**METHODS AND RESULTS:** We recruited 50 participants without cardiovascular disease from the Cardiac Aging Study conducted between 2014 and 2016. We performed transthoracic echocardiography imaging to measure cardiac structure indices such as left ventricular internal diameter end diastole index, left ventricular internal diameter end systole index, left ventricular mass index, and left atrial volume index, and retinal imaging to measure retinal vascular geometric indices including branching angle, curvature tortuosity, and fractal dimension. We applied multiple linear regressions to examine associations between indices of cardiac structure and retinal vascular geometry, adjusting for age, sex, body mass index, mean blood pressure, and comorbidity. The average age of all participants was 62.54 years old and slightly more than half were male (27; 54%). Each unit increase in a set of cardiac structure indices was associated with larger retinal arteriolar branching angle ( $\beta$  and 95% CI: for left ventricular internal diameter end systole index, 26.93°; 6.00–47.86; for left ventricular internal diameter end diastole index, 17.86°; 1.61–34.11; for left ventricular mass index, 0.39°; 0.10–0.67; for left atrial volume index, 0.91°; 0.24–1.58).

**CONCLUSIONS:** Adverse retinal arteriolar geometric morphology mirrored suboptimal cardiac structural alteration.

**Key Words:** cardiac structure ■ heart ■ retina ■ retinal microvasculature ■ retinal vascular geometry

The retina offers a unique yet noninvasive “window” to visualize retinal small vessels, and such microvascular morphology has been shown to reflect changes in general microcirculation *in vivo*.<sup>1</sup> Retinal arteriolar narrowing and venular widening has been widely suggested to be associated with cardiovascular risk factors (ie, high blood pressure, diabetes mellitus, and coronary artery disease),<sup>2–4</sup> subclinical alterations in cardiac structure,<sup>5–7</sup> and heart failure (HF).<sup>7,8</sup> For example, large-scale population-based, cross-sectional studies showed that changes in cardiac structure (ie, increased left ventricular [LV] mass, LV diameter, LV post wall thickness, and LV septum thickness and

decreased right ventricular mass and volume) were associated with retinal arteriolar narrowing and/or retinal venular widening among patients who had no history of physician-diagnosed cardiovascular disease (CVD).<sup>5,6</sup> Therefore, existing evidence leans toward the possibility that adverse microvascular alteration may underlie different stages of cardiac remodeling before developing symptomatic HF.<sup>9</sup> However, such findings are also largely confined to retinal vascular calibers, which only explain or reflect partial changes in the microcirculation.

In the past decade, emerging grading techniques have been developed to perform quantitative

Correspondence to: Ling-Jun Li, MD, PhD, Department of Obstetrics and Gynaecology, Yong Loo Lin School of Medicine, Singapore. 1E Kent Ridge Road, Level 12, Singapore 119228. Singapore Eye Research Institute, Singapore. The Academia, 20 College Road, Discovery Tower level 6, Singapore 169856. E-mail: queenie.li.l.j@gmail.com

Supplementary material for this article is available at <https://www.ahajournals.org/doi/suppl/10.1161/JAHA.119.014654>

\*Dr. Koh and Dr. Li are co-senior authors.

For Sources of Funding and Disclosures, see page 8.

© 2020 The Authors. Published on behalf of the American Heart Association, Inc., by Wiley. This is an open access article under the terms of the Creative Commons Attribution-NonCommercial-NoDerivs License, which permits use and distribution in any medium, provided the original work is properly cited, the use is non-commercial and no modifications or adaptations are made.

JAHA is available at: [www.ahajournals.org/journal/jaha](http://www.ahajournals.org/journal/jaha)

## CLINICAL PERSPECTIVE

### What Is New?

- In this study, we observed significant associations between subclinical changes in cardiac structure and suboptimal retinal arteriolar geometry among elderly subjects without prior history of cardiovascular disease.

### What Are the Clinical Implications?

- These findings indicated that retinal vascular geometry was associated with early-stage cardiac remodeling, and perhaps a useful noninvasive tool to help in further identifying patients with cardiac structural changes in addition to conventional tools (ie, magnetic resonance imaging and echography) that are reflective of cardiovascular disease risk.

## Nonstandard Abbreviations and Acronyms

<b>BMI</b>	body mass index
<b>CVD</b>	cardiovascular disease
<b>HF</b>	heart failure
<b>IVSD</b>	interventricular septum thickness at end diastole
<b>IVSS</b>	interventricular septum thickness at end systole
<b>LA</b>	left atrial
<b>LAVI</b>	left atrial volume index
<b>LV</b>	left ventricular
<b>LVEF</b>	left ventricular ejection fraction
<b>LVIDD</b>	left ventricular internal diameter at end diastole index
<b>LVDSI</b>	left ventricular internal diameter at end systole index
<b>LVM</b>	left ventricular mass index
<b>LVOTI</b>	left ventricular outflow tract index
<b>MAP</b>	mean arteriolar pressure

assessments on retinal vascular geometric measures that capture novel information on retinal vessels, such as branching angle, fractal dimension, and curvature tortuosity.<sup>10–13</sup> A body of research evidence has reported that retinal vascular geometric indices were associated with inflammation, endothelial dysfunction, and even microvascular and macrovascular disease.<sup>14,15</sup> Thus, such geometric measures may serve as a proxy of microvascular morphology besides retinal vascular caliber, and therefore, it is worth

exploring the changes in retinal vascular geometry in addition to caliber in relation to cardiac structural alteration, which might better explain the pathophysiological development of cardiac remodeling before the onset of CVD.

In this study of 50 community participants without prior CVD, we aimed to investigate the cross-sectional relationships between cardiac structure and retinal vascular geometry. We hypothesized that suboptimal cardiovascular structure (ie, increased LV mass index [LVM], larger left atrial [LA] size) would be associated with alterations in retinal vascular geometry (ie, higher retinal vascular curvature tortuosity, lower retinal vascular fractal dimension, and larger retinal vascular branching angle).

## METHODS

The data that support the findings of this study are available from the corresponding author upon reasonable request.

### Study Design and Study Participants

We recruited the participants from the Cardiac Aging Study, a prospective, hospital-based cohort conducted in Singapore between 2014 and 2016, which examined various characteristics and determinants of cardiovascular function in elderly adults.<sup>16,17</sup> We published the inclusion and exclusion criteria for Cardiac Aging Study in previous studies.<sup>16,17</sup> We further included Cardiac Aging Study participants who met the following criteria into this pilot study: (1) agreed to an additional retinal examination; and (2) had no self-reported history of clinically diagnosed cardio- or cerebrovascular disease (ie, coronary heart disease and stroke) and cancer. A total of 50 patients met the eligibility requirement. The study complied with the Declaration of Helsinki. All participants agreed and signed the written informed consent upon enrollment. The SingHealth Centralised Institutional Review Board (2014/628/C) approved the study protocol.

### Transthoracic Echocardiography Imaging—Assessments of Cardiac Structure

The echocardiographer performed echocardiography (ALOKA  $\alpha$ 10 with a 3.5 MHz probe, Hitachi Medical, Wallington, CT), using standard protocol that included 2-dimensional, M-mode, pulse Doppler and tissue Doppler imaging, in the standard parasternal and apical (apical 4-chamber, apical 2-chamber, and apical long) views, along with 3 recorded cardiac cycles. Using such Doppler images,

the echocardiographer subsequently measured interventricular septum thickness at end diastole (IVSD), interventricular septum thickness at end systole (IVSS), LV internal diameter at end diastole, LV internal diameter at end systole, LV posterior wall at end diastole, LV posterior wall at end systole, LV outflow tract, LA volume and LV ejection fraction (LVEF), according to the recommendations of the American Society of Echocardiography.<sup>18</sup> For all subjects, the same echocardiographer assessed measurements across three cardiac cycles and averaged the readings by adjusting them with the interbeat interval. The echocardiographer recorded the height and weight of the subject at the time of the study and calculated body surface area. The echocardiographer further calculated LV mass according to a necropsy-validated formula of LV mass (g)=0.8×(1.04×((septal thickness+LV internal diameter+posterior wall thickness)<sup>3</sup>−(LV internal diameter)<sup>3</sup>))+0.6,<sup>19</sup> and calculated LA volumes at end-systole from the apical 4-chamber view using the area-length method.<sup>20</sup> Finally, the echocardiographer calculated IVSD index, IVSS index, LV internal diameter at end diastole index (LVIDD), LV internal diameter at end systole index (LVIDS), LV posterior wall at end diastole index, LV posterior wall at end systole index, LV outflow tract index (LVOTI), LVMI and LA volume index (LAVI) as IVSD, IVSS, LV internal diameter at end diastole, LV internal diameter at end systole, LV posterior wall at end diastole, LV posterior wall at end systole, LV outflow tract, LV mass, and LA volume divided by body surface area, accordingly.

## Retinal Photography Assessments—Retinal Vascular Geometry

A trained photographer took the optic disc-centered and macular-centered retinal photographs of both eyes with pharmacological pupil dilation using a 45° non-mydratric retinal camera (Canon CR-1, 40D SLR digital retinal camera backing, Canon Inc, Tokyo, Japan).<sup>21</sup> A trained grader blinded to the patients' data graded both eyes' retinal images and assessed retinal vascular geometric indices quantitatively based on all vessels beyond 25 μm crossing through 0.5 to 2.0 disc diameters (zone C) from the optic disc margin, via a semiautomated computer-based program (Singapore I Vessel Assessment version 3.0, Singapore Eye Research Institute, Singapore), according to a standard protocol described elsewhere.<sup>10</sup> The Figure shows the Singapore I Vessel Assessment grading platform for all retinal vascular parameters. The same grader reanalyzed the vessels in 10% of the total retinal images, and intragrader correlation coefficient is consistently >80% across all retinal vascular geometric indices. All novel retinal vascular geometric indices included the following:

1. *Retinal vascular branching angle* was defined as the first angle subtended between 2 daughter vessels at each bifurcation.<sup>11</sup> We summarized the estimates as retinal arteriolar and venular branching angle, respectively.
2. *Retinal vascular curvature tortuosity* was defined as the integral of the curvature square along the path of the vessel, normalized by the total path length.<sup>12</sup> We summarized the estimates as retinal arteriolar

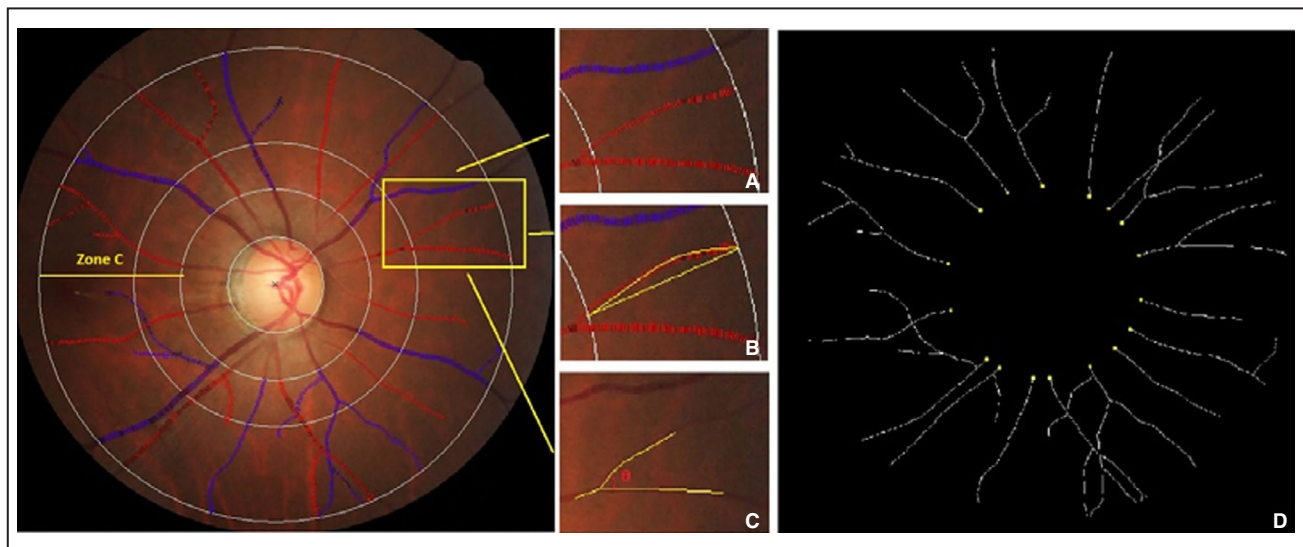


**Figure.** Singapore I Vessel Assessment grading platform for all retinal vascular parameters.

The far left retinal fundus photograph is generated from a computer-assisted program which is to assess retinal vascular parameters. All retinal arterioles and venules larger than 25 μm are marked and assessed within zone C that is within 0.5 to 2.0 optic disc diameter away from the margin of optic disc (highlighted in yellow). Retinal vascular caliber (A), retinal vascular tortuosity (B), retinal vascular branching angle (C), and retinal vascular fractal dimension (D) are shown, accordingly.

**Table 1. Characteristics of Study Participants**

Characteristics	Total (N=50)	Sex		P Value
		Male (n=27)	Female (n=23)	
Age, y	62.54 (11.74)	62.78 (11.62)	62.26 (12.13)	0.88
Ethnicity				
Chinese	50 (100)	27 (100)	23 (100)	...
History of comorbidity				
Hypertension, yes	16 (32.00)	10 (37.00)	6 (26.10)	0.55
Dyslipidemia, yes	20 (40.00)	12 (44.40)	8 (34.80)	0.57
Diabetes mellitus, yes	4 (8.00)	2 (7.40)	2 (8.70)	1.00
Combination of comorbidity				
Without any condition	23 (46.00)	10 (37.0)	13 (56.5)	0.26
With at least 1 condition	27 (54.00)	17 (63.0)	10 (43.5)	
Smoking status				
Never	34 (68.00)	13 (48.20)	21 (91.40)	0.01
Current smoker	5 (10.00)	4 (14.80)	1 (4.30)	
Past smoker	11 (22.00)	10 (37.00)	1 (4.30)	
BMI, kg/m <sup>2</sup>	23.93 (3.58)	25.17 (3.61)	22.46 (2.98)	0.01
Waist-to-hip ratio	0.87 (0.08)	0.90 (0.06)	0.82 (0.08)	<0.001
Blood pressure, mm Hg				
SBP	123.14 (17.99)	123.22 (16.10)	123.04 (20.35)	0.97
DBP	74.60 (10.08)	76.78 (9.70)	74.04 (10.12)	0.10
MAP	94.80 (11.24)	96.19 (9.36)	93.17 (13.15)	0.35
Cardiac structure indices				
IVSDI, cm	0.46 (0.07)	0.43 (0.06)	0.50 (0.07)	0.001
IVSSI, cm	0.73 (0.15)	0.70 (0.15)	0.77 (0.15)	0.07
LVIDDI, cm	2.68 (0.39)	2.57 (0.35)	2.80 (0.41)	0.04
LVIDSI, cm	1.54 (0.27)	1.46 (0.24)	1.63 (0.28)	0.03
LVPWDI, cm	0.44 (0.07)	0.42 (0.07)	0.46 (0.06)	0.08
LVPWSI, cm	0.87 (0.13)	0.85 (0.11)	0.89 (0.14)	0.21
LVOTI, cm	1.26 (0.12)	1.19 (0.11)	1.33 (0.10)	<0.001
LVMi, g/m <sup>2</sup>	67.94 (18.88)	69.96 (19.16)	65.57 (18.69)	0.42
LAVI, mL/m <sup>2</sup>	19.96 (7.94)	20.44 (7.20)	19.41 (8.88)	0.65
AOI, cm	1.80 (0.26)	1.82 (0.21)	1.77 (0.32)	0.55
LAI, cm	2.21 (0.38)	2.17 (0.39)	2.26 (0.36)	0.41
Cardiac function index				
LVEF (%)	72.96 (8.11)	73.75 (7.49)	72.03 (8.86)	0.46
Retinal vascular parameters				
CRAE, $\mu$ m	133.85 (11.51)	132.64 (11.81)	135.26 (11.23)	0.43
CRVE, $\mu$ m	199.14 (16.07)	199.15 (17.47)	196.96 (14.54)	0.64
DF-a, Df	1.19 (0.08)	1.19 (0.09)	1.20 (0.08)	0.71
DF-v, Df	1.21 (0.08)	1.21 (0.08)	1.21 (0.08)	0.88
CT-a ( $\times 10^{-5}$ units)	5.45 (4.27)	5.48 (5.15)	5.46 (3.07)	0.99
CT-v ( $\times 10^{-5}$ units)	7.79 (3.01)	7.57 (2.90)	8.05 (3.17)	0.58
BA-a, $^{\circ}$	69.74 (18.80)	70.22 (22.12)	69.19 (17.15)	0.86
BA-v, $^{\circ}$	76.62 (13.61)	73.75 (16.90)	80.00 (7.27)	0.11

Mean (SD) are presented for continuous variables and N (%) are presented for noncontinuous variables. AOI indicates aortic diameter index; BA-a, branching angle-arteriole; BA-v, branching angle-venule; BMI, body mass index; CRAE, central retinal arteriolar equivalent; CRVE, central retinal venular equivalent; CT-a, curvature tortuosity-arteriole; CT-v, curvature tortuosity-venule; DBP, diastolic blood pressure; DF-a, fractal dimension-arteriole; DF-v, fractal dimension-venule; IVSDI, interventricular septum thickness at end diastole index; IVSSI, interventricular septum thickness at end systole index; LAI, left atrium index; LAVI, left atrial volume index; LVEF, left ventricular ejection fraction; LVIDDI, left ventricular internal diameter at end diastole index; LVIDSI, left ventricular internal diameter at end systole index; LVMi, left ventricular mass index; LVOTI, left ventricular outflow tract index; LVPWDI, left ventricular posterior wall at end diastole index; LVPWSI, left ventricular posterior wall at end systole index; MAP, mean arterial blood pressure; and SBP, systolic blood pressure.

**Table 2. Associations Between Cardiac Structure Indices and Retinal Arteriolar Geometric Parameters**

Each Unit Increase in Echo Parameters	DF-a (Df) β (95% CI)	CT-a (x10 <sup>-5</sup> units) β (95% CI)	BA-a (°) β (95% CI)
<b>IVSS index</b>			
Model 1	-0.20 (-0.35 to -0.05)*	9.18 (1.34 to 17.02)*	-44.93 (-80.99 to -8.87)*
Model 2	-0.10 (-0.27 to 0.06)	11.86 (2.35 to 21.36)*	-32.68 (-76.00 to 10.64)
Model 3	-0.12 (-0.29 to 0.05)	11.46 (1.83 to 21.09)*	-28.08 (-72.40 to 16.24)
Model 4	-0.12 (-0.29 to 0.05)	11.27 (1.90 to 20.64)*	-29.02 (-71.86 to 13.83)
<b>IVSD index</b>			
Model 1	-0.34 (-0.65 to -0.04)*	11.41 (-4.96 to 27.78)	-54.60 (-130.33 to 21.12)
Model 2	-0.20 (-0.57 to 0.18)	0.77 (-2.70 to 4.25)	-15.65 (-115.09 to 83.78)
Model 3	-0.22 (-0.61 to 0.17)	14.40 (-8.28 to 37.08)	-3.90 (-105.66 to 97.86)
Model 4	-0.23 (-0.62 to 0.16)	15.68 (-6.36 to 37.71)	1.85 (-96.99 to 100.68)
<b>LVDDI</b>			
Model 1	-0.002 (-0.06 to 0.06)	0.84 (-2.33 to 4.00)	4.29 (-10.34 to 18.92)
Model 2	0.02 (-0.04 to 0.08)	0.77 (-2.70 to 4.25)	9.97 (-4.99 to 24.93)
Model 3	0.02 (-0.05 to 0.09)	-0.64 (-4.64 to 3.37)	19.03 (2.36 to 35.70)*
Model 4	0.02 (-0.05 to 0.09)	-0.91 (-4.82 to 3.00)	17.86 (1.61 to 34.11)*
<b>LVIDSI</b>			
Model 1	0.08 (-0.01 to 0.16)	-1.70 (-6.29 to 2.89)	21.57 (1.14 to 42.08)*
Model 2	0.06 (-0.02 to 0.14)	-1.75 (-6.72 to 3.23)	21.38 (0.43 to 42.33)*
Model 3	0.06 (-0.03 to 0.15)	-3.09 (-8.25 to 2.08)	28.68 (7.26 to 50.10)*
Model 4	0.06 (-0.03 to 0.15)	-3.53 (-8.55 to 1.49)	26.93 (6.00 to 47.86)*
<b>LVPWDI</b>			
Model 1	-0.31 (-0.65 to 0.03)	6.71 (-11.62 to 25.04)	-60.51 (-144.04 to 23.02)
Model 2	-0.06 (-0.43 to 0.31)	6.57 (-15.66 to 28.80)	-17.18 (-114.79 to 80.43)
Model 3	-0.08 (-0.47 to 0.31)	7.15 (-15.59 to 29.89)	-3.20 (-103.85 to 97.46)
Model 4	-0.08 (-0.47 to 0.31)	7.88 (-14.28 to 30.03)	0.18 (-97.47 to 97.82)
<b>LVPWSI</b>			
Model 1	-0.28 (-0.45 to -0.10)*	6.18 (-3.57 to 15.93)	-17.61 (-63.23 to 28.01)
Model 2	-0.17 (-0.36 to 0.02)	7.02 (-4.77 to 18.82)	13.39 (-38.92 to 65.69)
Model 3	-0.18 (-0.38 to 0.02)	5.56 (-6.45 to 17.57)	19.13 (-34.00 to 72.26)
Model 4	-0.18 (-0.38 to 0.02)	4.11 (-7.77 to 15.99)	12.14 (-40.08 to 64.36)
<b>LVOTI</b>			
Model 1	-0.21 (-0.39 to -0.03)*	10.06 (0.54 to 19.59)*	-66.00 (-107.98 to -24.01)*
Model 2	-0.20 (-0.42 to 0.02)	16.92 (4.08 to 29.76)*	-79.98 (-135.50 to -24.45)*
Model 3	-0.36 (-0.63 to -0.10)*	20.46 (4.68 to 36.23)*	-84.14 (-154.33 to -13.95)*
Model 4	-0.37 (-0.64 to -0.10)*	21.26 (6.06 to 36.47)*	-80.79 (-148.91 to -12.67)*
<b>LVMI</b>			
Model 1	0.00 (-0.001 to 0.001)	-0.01 (-0.08 to 0.05)	0.24 (-0.05 to 0.54)
Model 2	0.001 (0.00 to 0.002)	-0.02 (-0.09 to 0.05)	0.34 (0.05 to 0.63)*
Model 3	0.001 (0.00 to 0.002)	-0.04 (-0.11 to 0.04)	0.40 (0.10 to 0.69)*
Model 4	0.001 (0.00 to 0.002)	-0.04 (-0.11 to 0.03)	0.39 (0.10 to 0.67)*
<b>LAVI</b>			
Model 1	0.002 (-0.001 to 0.01)	-0.07 (-0.22 to 0.09)	0.57 (-0.13 to 1.28)
Model 2	0.003 (0.001 to 0.01)*	-0.08 (-0.25 to 0.08)	0.87 (0.19 to 1.55)*
Model 3	0.003 (0.001 to 0.01)*	-0.10 (-0.27 to 0.07)	0.99 (0.32 to 1.67)*
Model 4	0.003 (0.001 to 0.01)*	-0.12 (-0.28 to 0.04)	0.91 (0.24 to 1.58)*
<b>AOI</b>			
Model 1	-0.10 (-0.19 to -0.01)*	3.52 (-1.09 to 8.13)	-15.79 (-37.18 to 5.60)

(Continued)

**Table 2. Continued**

Each Unit Increase in Echo Parameters	DF-a (Df) β (95% CI)	CT-a (×10 <sup>-5</sup> units) β (95% CI)	BA-a (°) β (95% CI)
Model 2	-0.03 (-0.12 to 0.06)	4.02 (-1.48 to 9.51)	-4.51 (-29.09 to 20.08)
Model 3	-0.03 (-0.12 to 0.07)	3.85 (-1.65 to 9.34)	-5.51 (-30.21 to 19.19)
Model 4	-0.03 (-0.12 to 0.07)	3.55 (-1.83 to 8.93)	-7.02 (-30.97 to 16.93)
<b>LAI</b>			
Model 1	-0.08 (-0.13 to -0.02)*	3.45 (0.34 to 6.56)*	-24.59 (-37.92 to 11.26)
Model 2	-0.02 (-0.09 to 0.05)	4.84 (0.85 to 8.83)*	-22.64 (-39.95 to -5.33)*
Model 3	-0.04 (-0.12 to 0.04)	4.79 (0.33 to 9.25)*	-21.13 (-40.77 to -1.48)*
Model 4	-0.04 (-0.12 to 0.04)	4.49 (0.17 to 8.87)*	-22.81 (-41.64 to -3.97)*
<b>LVEF</b>			
Model 1	-0.003 (-0.01 to -0.001)*	0.11 (-0.03 to 0.26)	-0.80 (-1.45 to -0.15)*
Model 2	-0.001 (-0.004 to 0.002)	0.12 (-0.05 to 0.29)	-0.56 (-1.30 to 0.17)
Model 3	-0.001 (-0.004 to 0.002)	0.11 (-0.06 to 0.28)	-0.51 (-1.25 to 0.24)
Model 4	-0.001 (-0.004 to 0.002)	0.12 (-0.05 to 0.28)	-0.46 (-1.18 to 0.27)

Model 1 unadjusted model. Model 2 adjusted for sex and age. Model 3 adjusted for sex, age, MAP and BMI. Model 4 adjusted for sex, age, MAP, BMI and combination of co-morbidity. AOI indicates aortic diameter index; BA-a, branching angle-arteriole; CT-a, curvature tortuosity-arteriole; DF-a, fractal dimension-arteriole; IVSD, interventricular septum thickness at end diastole; IVSS, interventricular septum thickness at end systole; LAI, left atrium index; LAVI, left atrial volume index; LVEF, left ventricular ejection fraction; LVIDDl, left ventricular internal diameter at end diastole index; LVIDSI, left ventricular internal diameter at end systole index; LVMI, left ventricular mass index; LVOTI, left ventricular outflow tract index; LVPWDl, left ventricular posterior wall at end diastole index; and LVPWSI, left ventricular posterior wall at end systole index.

\*Beta and 95% CI are presented in the table, and values with statistical significance ( $P < 0.05$ ) are highlighted.

curvature tortuosity and retinal venular curvature tortuosity, representing the average tortuosity of arterioles and venules of the eye, respectively.

3. *Retinal vascular fractal dimension* was calculated from the outlined retinal vessels using the “box-counting method,” which divided each photograph into a series of squares of various side lengths, and fractal dimension was defined as the gradient of logarithms of the number of boxes and the size of those boxes.<sup>13</sup> Retinal vascular fractal dimension quantified the complexity of the branching pattern of the retinal vascular tree, and it was represented by a ratio. We summarized the estimates as retinal arteriolar and venular fractal dimension, respectively.

## Covariates

We defined self-reported hypertension by current use of antihypertensive drugs or physician-diagnosed hypertension, diabetes mellitus by current use of antidiabetic agents or physician-diagnosed diabetes mellitus, and dyslipidemia by current use of lipid-lowering agents or physician-diagnosed dyslipidemia. We defined smoking history as never or current smoker or past smoker. Furthermore, trained personnel obtained systolic blood pressure and diastolic blood pressure, height, and weight from medical records during the same visit, and calculated mean arteriolar pressure (MAP) as the sum of one-third of systolic blood pressure and two-thirds of diastolic blood pressure, and also body mass index (BMI) as

weight in kilograms divided by the square of height in meters.

## Statistical Analysis

We used means and SD to describe age, BMI, MAP, cardiac structure and retinal vascular geometric indices, and counts and percentages to describe sex, smoking status, and history of co-morbidity. We conducted multiple linear regression models to assess the associations between cardiac structure and function and retinal vascular geometry. According to prior publications,<sup>22,23</sup> we chose age, sex, BMI, MAP, and any history of comorbidity as potential confounders. We applied 4 models in the multiple linear regression: Model 1, unadjusted; Model 2, adjusted for age and sex; Model 3, Model 2 and additionally adjusting for MAP and BMI; Model 4, Model 3 and additionally adjusting for history of comorbidity. For all analyses, we defined a significant  $P$  value (2-tailed) as 0.05. We performed all statistical analyses using SPSS (SPSS, version 23.0, IBM, Armonk, NY).

## RESULTS

The mean and SD in age of our participants ( $N=50$ ) were  $62.54 \pm 11.74$  years. The majority of participants had reported history of hypertension (32%), dyslipidemia (40%), and diabetes mellitus (8%), and slightly more than half of them were male (54%) (Table 1). The mean and SD of major cardiac structural indices

including LVDDI, LVDSI, LVMI, LAVI, and LVEF were  $2.68 \pm 0.39$  cm,  $1.54 \pm 0.27$  cm,  $67.94 \pm 18.88$  g/m<sup>2</sup>,  $19.96 \pm 7.94$  mL/m<sup>2</sup>, and  $72.96 \pm 8.11\%$ , respectively (Table 1). The mean and SD of retinal arteriolar fractal dimension, retinal venular fractal dimension, retinal arteriolar curvature tortuosity, retinal venular curvature tortuosity, retinal arteriolar branching angle, and retinal venular branching angle were  $1.19 \pm 0.08$  Df,  $1.21 \pm 0.08$  Df,  $5.45 \pm 4.27$  ( $\times 10^{-5}$  units),  $7.79 \pm 3.01$  ( $\times 10^{-5}$  units),  $69.74 \pm 18.80^\circ$ , and  $76.62 \pm 13.61^\circ$ , respectively (Table 1). Compared with the females ( $n=23$ ), the males had more vascular risk factors (ie, more ever smokers, larger waist-to-hip ratio, and higher BMI) (Table 1). Additionally, the males had smaller IVSD index, IVSS index, LVDDI, LV posterior wall at end diastole index, LV posterior wall at end systole index, and LVOTI than the females (Table 1).

After adjusting for age, sex, MAP, BMI, and combination of co-morbidity, significant associations were observed between a series of cardiac structure indices and larger retinal arteriolar branching angle ( $\beta$  and 95% CI: for LVDSI,  $26.93^\circ$ ,  $6.00$ – $47.86$ ; for LVDDI,  $17.86^\circ$ ,  $1.61$ – $34.11$ ; for LVMI,  $0.39^\circ$ ,  $0.10$ – $0.67$ ; for LAVI,  $0.91^\circ$ ,  $0.24$ – $1.58$ ) and higher retinal arteriolar fractal dimension (for LAVI,  $0.003$  Df,  $0.001$ – $0.01$ ) (Table 2). Each unit increase in LVOTI was associated with smaller retinal arteriolar branching angle ( $-80.89^\circ$ ,  $-148.91$  to  $-12.67$ ), increased retinal arteriolar curvature tortuosity ( $21.26 \times 10^{-5}$  units,  $6.06$ – $36.47$ ), and lower retinal arteriolar fractal dimension ( $-0.37$  Df,  $-0.64$  to  $-0.10$ ) (Table 2). However, no associations were observed between other cardiac structure indices, LVEF, and retinal arteriolar geometric parameters. In addition, significant association of LAVI with lower retinal venular curvature tortuosity ( $-0.11$ ,  $-0.22$  to  $-0.004$ ), IVSS index with smaller retinal venular branching angle ( $-34.28^\circ$ ,  $-64.41$  to  $-4.16$ ), IVSD index with increased retinal venular curvature tortuosity ( $17.94 \times 10^{-5}$  units,  $3.15$ – $32.73$ ), and LVOTI with lower retinal venular fractal dimension ( $-0.27$  Df,  $-0.54$  to  $-0.003$ ) were observed (Table S1). No associations were observed between other cardiac structure indices, LVEF, and retinal venular geometric parameters.

Table S2 shows that each unit increase in LVOTI was associated with narrowing central retinal arteriolar equivalent after adjusted the potential confounders ( $-41.67$   $\mu$ m,  $-82.19$  to  $-1.13$ ). No significant associations between other cardiac structure indices, LVEF, and retinal vascular calibers were observed.

## DISCUSSION

In this study, we observed significant associations between subclinical changes in cardiac structure and suboptimal retinal arteriolar geometry among elderly

subjects without prior history of CVD. Our findings suggest that a series of adverse changes in cardiac structure indices (ie, enlarged LVDDI, LVDSI, LVMI, and LAVI and smaller LVOTI) were associated with retinal arteriolar geometric abnormalities (ie, larger branching angle, higher fractal dimension, and lower curvature tortuosity), but not with retinal vascular caliber. Our findings suggest that subclinical alterations in cardiac structure were linked to suboptimal retinal arteriolar geometry instead of retinal arteriolar narrowing, supporting the hypothesis that arteriolar changes in geometry might be more informative about left atrial and ventricular remodeling, compared with retinal arteriolar narrowing.

The retina is a site where microcirculation can be imaged directly, providing a unique opportunity to study *in vivo* the morphology of human microcirculation.<sup>1</sup> Microvascular disease has been hypothesized to influence HF as well as subclinical cardiac remodeling.<sup>9</sup> Changes in retinal vascular calibers, which manifest as narrower retinal arteriolar caliber, have also been linked with suboptimal cardiac structure and even HF.<sup>5–8</sup> However, these studies largely have been confined to retinal vascular caliber. Retinal vascular geometry (ie, branching angle, fractal dimension, and curvature tortuosity), which better reflects the complexity of retinal vasculature and provides more insight into optimal microcirculation,<sup>11–13</sup> has not yet been explored in its relationship to cardiac remodeling.

Cardiac remodeling can be described as a physiologic and pathologic condition that may occur after myocardial infarction, pressure overload (ie, aortic stenosis, hypertension), inflammatory heart muscle disease (ie, myocarditis), idiopathic dilated cardiomyopathy, or volume overload (ie, valvular regurgitation).<sup>24</sup> LV remodeling is the rapidest occurrence and progression in cardiac remodeling.<sup>25</sup> Hence, we first explore the relationship of LV structure over other cardiac structural parameters with retinal vascular geometry among patients without CVD. Our data suggest that LV structure indices (ie, increments in LVMI, LVDDI, and LVDSI and decrement in LVOTI) were significantly associated with a series of suboptimal retinal arteriolar geometric morphology, namely, larger retinal arteriolar branching angle, lower retinal arteriolar curvature tortuosity, and higher retinal arteriolar fractal dimension. It could be because the left ventricle is pumping the blood to the arterial system directly, so that arterioles are more sensitive to the LV alterations. However, further studies with larger samples are needed to validate these observations.

LA remodeling caused by high filling pressures represents a crucial point of transition from asymptomatic to symptomatic HF.<sup>26</sup> Importantly, LA enlargement and elevated LA pressures are commonly associated with

HF with preserved ejection fraction.<sup>27</sup> We observed that higher LAVI, commonly used to describe LA enlargement, was significantly associated with larger retinal arteriolar branching angle and higher retinal arteriolar fractal dimension.

It is suggested that a larger retinal branching angle reflects greater workload and energy spent in maintaining efficient blood circulation, and reportedly linked to disrupted blood flow, and endothelial damage.<sup>14</sup> As for arteriolar tortuosity, prior evidence has showed that lower arteriolar tortuosity was related to coronary artery disease, indicating endothelial dysfunction and impairment of perfusion or oxygenation at the level of microcirculation.<sup>4</sup> In turn, higher retinal arteriolar fractal dimension may be reflective of the microvascular remodeling before any characteristic vasculopathy manifests.<sup>15</sup> Hypothetically, alterations in LV and LA structure might be driven by similar mechanisms such as microvascular dysfunction.<sup>9</sup> Interestingly, we found little evidence on associations between cardiac structure and retinal venular measures, which indicated that changes in retinal arterioles are more sensitive to subclinical alterations in LV and LA structure than venules. Such findings are similar to the findings of large arterial function and structure, and hypertension, in which changes in arterioles are also prominent.<sup>28,29</sup> One possible explanation might be that adverse changes of venules may have an adaptive response, and this adaption would break down when cardiometabolic disease becomes overt, leading to suboptimal changes in venules.<sup>30</sup> Further studies are clearly required to verify our hypothesis and elucidate the underlying mechanism.

Our study reports novel associations between cardiac structure and retinal vascular geometry. In spite of this, we acknowledge the limitations of our study. First, our sample size limited the statistical power detect all possible associations. Thus, further studies with larger samples are warranted to confirm our findings. Second, we did not correct our findings for multiple testing due to sample size limitation. Nevertheless, the pattern of associations we observed in a set of similar outcomes (ie, significant associations for retinal arteriolar geometric morphology) was consistent. Third, even though we corrected for multiple covariates, residual confounding by other unmeasured confounders including alcohol consumption, socioeconomic status, and endothelial dysfunction biomarkers is still possible. Fourth, some cardiac measurements (ie, strains, strain rate) that have been shown to be predictive of CVD were not investigated in this study.<sup>31,32</sup> Fifth, the study was performed in a sample of elderly Chinese subjects, and thus the findings may not be applicable to individuals of other ethnic groups or ages. Sixth, the cross-sectional nature of our study design precludes any inferences regarding the temporal nature of the

observed associations. Future longitudinal follow-up of these participants may provide greater insights into the relationship between cardiac structure and retinal vascular geometry.

In conclusion, our results suggest that subclinical alterations in cardiac structure were linked with sub-optimal retinal arteriolar geometry, supporting the hypothesis that arteriolar changes might underlie the pathophysiological mechanism of cardiac remodeling on the left atrium and ventricle. However, because of the small sample size and scarcity of reports on this topic, further longitudinal studies with larger samples with various cardiac parameters (ie, strains, strains rate) are needed to verify the relationships between cardiac remodeling and abnormal microvascular morphology.

## ARTICLE INFORMATION

Received September 16, 2019; accepted February 11, 2020.

### Affiliations

From the Guangzhou Key Laboratory of Environmental Pollution and Health Assessment, Guangdong Provincial Key Laboratory of Food, Nutrition and Health, Department of Medical Statistics and Epidemiology, School of Public Health (L.H., W.-Q.C.) and Department of Information Management, Xinhua College (W.-Q.C.), Sun Yat-sen University, Guangzhou, China; Division of Chronic Disease Research Across the Lifecourse, Department of Population Medicine, Harvard Medical School and Harvard Pilgrim Health Care Institute, Boston, MA (I.M.A.); National Heart Centre Singapore, Singapore (L.L.Y.T., A.S.K., L.-J.L.); Duke-NUS Medical School, Singapore (L.L.Y.T., A.S.K.); Division of Obstetrics and Gynecology, KK Women's and Children's Hospital, Singapore (T.Y.W.); Obstetrics and Gynecology Academic Clinical Program, Duke-NUS Medical School, Singapore (T.Y.W.); Singapore Eye Research Institute, Singapore National Eye Centre, Singapore (T.Y.W., L.-J.L.); Department of Obstetrics and Gynecology, Yong Loo Lin School of Medicine, Singapore (L.-J.L.).

### Acknowledgments

None.

Author contributions: Drs Teo, Koh, Wong, and Li acquired the data and designed and conducted the research; Drs Huang, Aris, and Chen analyzed the data and drafted the manuscript; Drs Huang, Koh, and Li had primary responsibility for the final content; Drs Aris, Koh, and Li critically revised the manuscript for important intellectual content; and all authors read and approved the final manuscript.

### Sources of Funding

This study was funded by the Singapore National Medical Research Council of Singapore (NMRC/TA/0031/2015, MOH-000153), Hong Leong Foundation, Duke-NUS Medical School, Estate of Tan Sri Khoo Teck Puat, and the SingHealth Foundation. Dr Li is supported by the Singapore National Medical Research Council Transition Award (NMRC TA/0027/2014).

### Disclosures

None.

### Supplementary Material

Tables S1–S2

## REFERENCES

- Dumitrescu AG, Voinea L, Badarau IA, Paun VA, Schowe M, Ciuluvica R. Update on retinal vascular caliber. *Rom J Ophthalmol*. 2017;61:171–180.
- Ding J, Wai KL, McGeechan K, Ikram MK, Kawasaki R, Xie J, Klein R, Klein BB, Cotch MF, Wang JJ, et al. Retinal vascular caliber and the

- development of hypertension: a meta-analysis of individual participant data. *J Hypertens*. 2014;32:207–215.
3. Sabanayagam C, Lye WK, Klein R, Klein BE, Cotch MF, Wang JJ, Mitchell P, Shaw JE, Selvin E, Sharrett AR, et al. Retinal microvascular calibre and risk of diabetes mellitus: a systematic review and participant-level meta-analysis. *Diabetologia*. 2015;58:2476–2485.
  4. Wang SB, Mitchell P, Liew G, Wong TY, Phan K, Thiagalingam A, Joachim N, Burlutsky G, Gopinath B. A spectrum of retinal vasculature measures and coronary artery disease. *Atherosclerosis*. 2018;268:215–224.
  5. Cheung N, Bluemke DA, Klein R, Sharrett AR, Islam FM, Cotch MF, Klein BE, Criqui MH, Wong TY. Retinal arteriolar narrowing and left ventricular remodeling: the Multi-Ethnic Study of Atherosclerosis. *J Am Coll Cardiol*. 2007;50:48–55.
  6. Chyou AC, Klein BEK, Klein R, Barr RG, Cotch MF, Praestgaard A, Wong TY, Lima J, Bluemke DA, Kawut S. Retinal vascular changes and right ventricular structure and function: the MESA-Right Ventricle and MESA-Eye studies. *Pulm Circ*. 2019;9:2045894018819781.
  7. Seidemann SB, Claggett B, Bravo PE, Gupta A, Farhad H, Klein BE, Klein R, Di Carli M, Solomon SD. Retinal vessel calibers in predicting long-term cardiovascular outcomes: the Atherosclerosis Risk in Communities study. *Circulation*. 2016;134:1328–1338.
  8. Chandra A, Seidemann SB, Claggett BL, Klein BE, Klein R, Shah AM, Solomon SD. The association of retinal vessel calibers with heart failure and long-term alterations in cardiac structure and function: the Atherosclerosis Risk in Communities (ARIC) Study. *Eur J Heart Fail*. 2019;21:1207–1215.
  9. Xu Z, Gu HP, Gu Y, Sun W, Yu K, Zhang XW, Kong XQ. Increased index of microcirculatory resistance in older patients with heart failure with preserved ejection fraction. *J Geriatr Cardiol*. 2018;15:687–694.
  10. Cheung CY, Lamoureux E, Ikram MK, Sasongko MB, Ding J, Zheng Y, Mitchell P, Wang JJ, Wong TY. Retinal vascular geometry in Asian persons with diabetes and retinopathy. *J Diabetes Sci Technol*. 2012;6:595–605.
  11. Zamir M. Optimality principles in arterial branching. *J Theor Biol*. 1976;62:227–251.
  12. Cheung CY, Zheng Y, Hsu W, Lee ML, Lau QP, Mitchell P, Wang JJ, Klein R, Wong TY. Retinal vascular tortuosity, blood pressure, and cardiovascular risk factors. *Ophthalmology*. 2011;118:812–818.
  13. Cheung CY, Thomas GN, Tay W, Ikram MK, Hsu W, Lee ML, Lau QP, Wong TY. Retinal vascular fractal dimension and its relationship with cardiovascular and ocular risk factors. *Am J Ophthalmol*. 2012;154:663–674.e1.
  14. Stanton AV, Wasan B, Cerutti A, Ford S, Marsh R, Sever PP, Thom SA, Hughes AD. Vascular network changes in the retina with age and hypertension. *J Hypertens*. 1995;13:1724–1728.
  15. Yau JW, Kawasaki R, Islam FM, Shaw J, Zimmet P, Wang JJ, Wong TY. Retinal fractal dimension is increased in persons with diabetes but not impaired glucose metabolism: the Australian Diabetes, Obesity and Lifestyle (AusDiab) study. *Diabetologia*. 2010;53:2042–2045.
  16. Hankin JH, Stram DO, Arakawa K, Park S, Low SH, Lee HP, Yu MC. Singapore Chinese Health Study: development, validation, and calibration of the quantitative food frequency questionnaire. *Nutr Cancer*. 2001;39:187–195.
  17. Koh AS, Gao F, Leng S, Kovalik JP, Zhao X, Tan RS, Fridianto KT, Ching J, Chua SJ, Yuan JM, et al. Dissecting clinical and metabolomics associations of left atrial phasic function by cardiac magnetic resonance feature tracking. *Sci Rep*. 2018;8:8138.
  18. Lang RM, Bierig M, Devereux RB, Flachskampf FA, Foster E, Pellikka PA, Picard MH, Roman MJ, Seward J, Shanewise J, et al. Recommendations for chamber quantification. *Eur J Echocardiogr*. 2006;7:79–108.
  19. Devereux RB, Alonso DR, Lutas EM, Gottlieb GJ, Campo E, Sachs I, Reichek N. Echocardiographic assessment of left ventricular hypertrophy: comparison to necropsy findings. *Am J Cardiol*. 1986;57:450–458.
  20. Lester SJ, Ryan EW, Schiller NB, Foster E. Best method in clinical practice and in research studies to determine left atrial size. *Am J Cardiol*. 1999;84:829–832.
  21. Wong TY, Klein R, Islam FM, Cotch MF, Folsom AR, Klein BE, Sharrett AR, Shea S. Diabetic retinopathy in a multi-ethnic cohort in the United States. *Am J Ophthalmol*. 2006;141:446–455.
  22. Tanai E, Frantz S. Pathophysiology of heart failure. *Compr Physiol*. 2015;6:187–214.
  23. Dharmarajan K, Rich MW. Epidemiology, pathophysiology, and prognosis of heart failure in older adults. *Heart Fail Clin*. 2017;13:417–426.
  24. Cohn JN, Ferrari R, Sharpe N. Cardiac remodeling—concepts and clinical implications: a consensus paper from an international forum on cardiac remodeling. Behalf of an International Forum on Cardiac Remodeling. *J Am Coll Cardiol*. 2000;35:569–582.
  25. Korup E, Dalsgaard D, Nyvad O, Jensen TM, Toft E, Bering J. Comparison of degrees of left ventricular dilation within 3 hours and up to 6 days after onset of first acute myocardial infarction. *Am J Cardiol*. 1997;80:449–453.
  26. Hohendanner F, Messroghli D, Bode D, Blaschke F, Parwani A, Boldt LH, Heinzel FR. Atrial remodelling in heart failure: recent developments and relevance for heart failure with preserved ejection fraction. *ESC Heart Fail*. 2018;5:211–221.
  27. Almeida P, Rodrigues J, Lourenco P, Maciel MJ, Bettencourt P. Left atrial volume index is critical for the diagnosis of heart failure with preserved ejection fraction. *J Cardiovasc Med (Hagerstown)*. 2018;19:304–309.
  28. Wang SB, Mitchell P, Plant AJ, Chiha J, Phan K, Liew G, Thiagalingam A, Kovoor P, Burlutsky G, Gopinath B. Hypertension is associated with narrower retinal arteriolar calibre in persons with and without coronary artery disease. *J Hum Hypertens*. 2016;30:761–765.
  29. Liu M, Wake M, Wong TY, He M, Xiao Y, Burgner DP, Lycett K. Associations of retinal microvascular caliber with intermediate phenotypes of large arterial function and structure: a systematic review and meta-analysis. *Microcirculation*. 2019;26:e12557.
  30. Wang JJ, Liew G, Klein R, Rochtchina E, Knudtson MD, Klein BE, Wong TY, Burlutsky G, Mitchell P. Retinal vessel diameter and cardiovascular mortality: pooled data analysis from two older populations. *Eur Heart J*. 2007;28:1984–1992.
  31. Santos-Gallego CG, Requena-Ibanez JA, San Antonio R, Ishikawa K, Watanabe S, Picatoste B, Flores E, Garcia-Ropero A, Sanz J, Hajjar RJ, et al. Empagliflozin ameliorates adverse left ventricular remodeling in nondiabetic heart failure by enhancing myocardial energetics. *J Am Coll Cardiol*. 2019;73:1931–1944.
  32. Park JJ, Park JB, Park JH, Cho GY. Global longitudinal strain to predict mortality in patients with acute heart failure. *J Am Coll Cardiol*. 2018;71:1947–1957.

# **SUPPLEMENTAL MATERIAL**

**Table S1. Associations between Cardiac Structure Indices and Retinal Venular Geometric Parameters.**

Each unit increase in echo parameters	DF-v (Df) Beta (95%CI)	CT-v (x 10 <sup>5</sup> units) Beta (95%CI)	BA-v (degree) Beta (95%CI)
<b>IVSSI</b>			
Model 1	<b>-0.17 (-0.32, -0.03)</b>	3.37 (-2.38, 9.11)	-18.13 (-43.96, 7.70)
Model 2	-0.06 (-0.22, 0.10)	5.39 (-1.53, 12.31)	<b>-37.92 (-67.24, -8.60)</b>
Model 3	-0.06 (-0.23, 0.11)	5.13 (-1.96, 12.21)	<b>-34.41 (-64.21, -4.60)</b>
Model 4	-0.06 (-0.23, 0.11)	4.97 (-1.85, 11.79)	<b>-34.28 (-64.41, -4.16)</b>
<b>IVSDI</b>			
Model 1	<b>-0.33 (-0.62, -0.03)</b>	9.98 (-1.41, 21.38)	5.94 (-47.21, 59.09)
Model 2	-0.10 (-0.46, 0.26)	<b>17.96 (2.95, 32.97)</b>	-33.28 (-103.01, 36.44)
Model 3	-0.09 (-0.47, 0.29)	<b>16.89 (1.35, 32.43)</b>	-22.31 (-93.21, 48.58)
Model 4	-0.09 (-0.47, 0.29)	<b>17.94 (3.15, 32.73)</b>	-23.26 (-94.98, 48.26)
<b>LVIDDI</b>			
Model 1	-0.01 (-0.07, 0.04)	0.02 (-2.21, 2.25)	-2.68 (-12.74, 7.39)
Model 2	0.01 (-0.04, 0.07)	-0.02 (-2.46, 2.42)	-6.36 (-16.98, 4.26)
Model 3	0.03 (-0.04, 0.09)	-0.95 (-3.77, 1.88)	-2.62 (-14.94, 9.70)
Model 4	0.03 (-0.04, 0.09)	-1.17 (-3.89, 1.54)	-2.44 (-14.93, 10.05)
<b>LVIDSI</b>			
Model 1	0.06 (-0.02, 0.14)	-0.62 (-3.86, 2.62)	3.22 (-11.44, 17.88)
Model 2	0.05 (-0.03, 0.13)	-1.15 (-4.63, 2.34)	0.02 (-15.47, 15.50)
Model 3	0.06 (-0.02, 0.14)	-1.91 (-5.59, 1.76)	4.68 (-11.44, 20.80)
Model 4	0.06 (-0.02, 0.15)	-2.27 (-5.80, 1.26)	5.02 (-11.32, 21.36)
<b>LVPWDI</b>			
Model 1	<b>-0.35 (-0.68, -0.03)</b>	2.25 (-10.71, 15.20)	-17.92 (-76.37, 110.39)
Model 2	-0.09 (-0.45, 0.26)	4.33 (-11.26, 19.91)	-50.20 (-117.74, 17.32)
Model 3	-0.09 (-0.46, 0.28)	4.68 (-11.44, 20.80)	-43.42 (-112.61, 25.78)
Model 4	-0.09 (-0.47, 0.28)	5.27 (-10.24, 20.78)	-43.98 (-113.89, 25.93)
<b>LVPWSI</b>			
Model 1	<b>-0.19 (-0.37, -0.02)</b>	0.36 (-6.61, 7.34)	-17.72 (-48.86, 13.42)
Model 2	-0.04 (-0.23, 0.15)	1.40 (-6.98, 9.78)	-35.96 (-71.50, -0.42)
Model 3	-0.04 (-0.24, 0.16)	0.50 (-8.10, 9.09)	-31.62 (-67.76, 4.53)
Model 4	-0.03 (-0.24, 0.17)	-0.77 (-9.12, 7.59)	-31.16 (-68.12, 5.79)
<b>LVOTI</b>			
Model 1	<b>-0.24 (-0.41, -0.07)</b>	4.84 (-2.03, 11.71)	-3.74 (-35.44, 27.96)
Model 2	-0.20 (-0.41, 0.02)	8.29 (-1.05, 17.63)	-37.54 (-78.78, 3.70)
Model 3	<b>-0.27 (-0.53, -0.002)</b>	9.66 (-1.99, 21.31)	-25.33 (-77.04, 26.37)
Model 4	<b>-0.27 (-0.54, -0.003)</b>	10.30 (-0.84, 21.44)	-25.94 (-78.21, 26.34)
<b>LVMI</b>			
Model 1	0.00 (-0.001, 0.002)	-0.01 (-0.06, 0.03)	-0.06 (-0.27, 0.15)
Model 2	0.001 (0.00, 0.002)	-0.01 (-0.06, 0.04)	-0.05 (-0.27, 0.16)
Model 3	0.001 (0.00, 0.002)	-0.02 (-0.07, 0.03)	-0.02 (-0.24, 0.20)
Model 4	0.001 (0.00, 0.002)	-0.02 (-0.07, 0.03)	-0.02 (-0.24, 0.21)
<b>LAVI</b>			
Model 1	0.001(-0.002, 0.004)	-0.09 (-0.20, 0.02)	-0.11 (-0.60, 0.39)
Model 2	0.002 (0.00, 0.01)	-0.09 (-0.20, 0.03)	-0.12 (-0.63, 0.39)
Model 3	0.002 (0.00, 0.01)	-0.10 (-0.21, 0.02)	-0.04 (-0.56, 0.48)
Model 4	0.002 (0.00, 0.01)	<b>-0.11 (-0.22, -0.004)</b>	-0.03 (-0.56, 0.50)
<b>AOI</b>			
Model 1	<b>-0.09 (-0.17,-0.01)</b>	1.38 (-1.92, 4.68)	-0.59 (-15.63, 14.44)
Model 2	-0.02 (-0.11, 0.07)	2.63 (-1.24, 6.49)	-1.62 (-19.03, 15.79)
Model 3	-0.02 (-0.11, 0.07)	2.54 (-1.37, 6.44)	-2.02 (-19.34, 15.29)
Model 4	-0.02 (-0.11, 0.07)	2.29 (-1.49, 6.06)	-1.81 (-19.34, 15.72)
<b>LAI</b>			
Model 1	<b>-0.09 (-0.14, -0.04)</b>	1.36 (-0.90, 3.63)	-7.89 (-18.03, 2.25)
Model 2	-0.04 (-0.11, 0.03)	2.71 (-0.15, 5.57)	<b>-16.60 (-28.78, -4.42)</b>
Model 3	-0.04 (-0.12, 0.03)	2.69 (-0.53, 5.91)	<b>-14.47 (-28.25, -0.69)</b>
Model 4	-0.43 (-0.12, 0.03)	2.44 (-0.68, 5.56)	<b>-14.33 (-28.31, -0.35)</b>
<b>LVEF</b>			
Model 1	<b>-0.003 (-0.01, -0.001)</b>	0.02 (-0.08, 0.13)	-0.30 (-0.77, 0.17)
Model 2	-0.001 (-0.004, 0.002)	0.05 (-0.07, 0.17)	-0.39 (-0.92, 0.13)

Model 3	-0.001 (-0.004, 0.001)	0.04 (-0.08, 0.16)	-0.33 (-0.86, 0.19)
Model 4	-0.002 (-0.004, 0.001)	0.05 (-0.07, 0.17)	-0.34 (-0.87, 0.19)

IVSSI: interventricular septum thickness at end systole index; IVSDI: interventricular septum thickness at end diastole index; LVIDDI: left ventricular internal diameter at end diastole index; LVIDSI: left ventricular internal diameter at end systole index; LVPWDI: left ventricular posterior wall at end diastole index; LVPWSI: left ventricular posterior wall at end systole index; LVOTI: left ventricular outflow tract index; LVMI: left ventricular mass index; LAVI: left atrial volume index; AOI: aortic diameter index; LAI: left atrium index; LVEF: left ventricular ejection fraction; DF-v: fractal dimension-venule; CT-v: curvature tortuosity-venule; BA-v: branching angle-venule.

Beta and 95%CI are presented in the table, and values with statistically significance ( $p < 0.05$ ) are highlighted in boldface font.

Model 1 unadjusted model

Model 2 adjusted for sex and age

Model 3 adjusted for sex, age, MAP and BMI

Model 4 adjusted for sex, age, MAP, BMI and history of co-morbidity

**Table S2. Associations between Cardiac Structure Indices and Retinal Vascular Calibers.**

Each unit increase in echo parameters	CRAE (μm)				CRVE (μm)			
	Beta (95%CI)				Beta (95%CI)			
	Model 1	Model 2	Model 3	Model 4	Model 1	Model 2	Model 3	Model 4
IVSSI	3.42 (-8.84, 25.69)	11.98 (-14.45, 38.40)	13.80 (-11.31, 38.92)	13.63 (-11.68, 38.94)	-17.74 (-48.42, 12.95)	4.10 (-31.45, 39.66)	9.75 (-23.89, 43.39)	9.81 (-24.23, 43.86)
IVSDI	12.83 (-31.98, 57.64)	34.08 (-24.85, 93.00)	31.17 (-25.46, 87.80)	32.39 (-24.68, 89.47)	-31.52 (-93.62, 30.59)	22.29 (-57.21, 101.79)	27.52 (-48.16, 103.20)	27.23 (-49.49, 103.96)
LVIDDI	7.43 (-0.82, 15.69)	9.03 (0.27, 17.79)	9.39 (-0.15, 18.93)	9.20 (-0.45, 18.85)	-4.29 (-16.14, 7.56)	-0.05 (-12.27, 12.17)	1.20 (-11.99, 14.40)	1.29 (-12.10, 14.68)
LVIDSI	9.61 (-2.49, 21.72)	7.92 (-5.02, 20.86)	7.85 (-4.98, 20.68)	7.53 (-5.46, 20.52)	-5.92 (-23.18, 11.34)	-8.40 (-25.77, 8.97)	-6.90 (-24.08, 10.27)	-6.83 (-24.28, 10.63)
LVPWDI	-5.04 (-54.63, 44.55)	7.96 (-50.70, 66.62)	22.38 (-33.53, 79.20)	23.51 (-33.27, 80.29)	-61.24 (-128.18, 5.71)	-23.28 (-101.31, 54.74)	1.03 (-74.28, 76.34)	0.81 (-75.45, 77.06)
LVPWSI	2.02 (-24.65, 28.70)	12.64 (-18.64, 43.92)	9.77 (-20.24, 39.78)	8.55 (-22.03, 39.13)	-10.07 (-47.20, 27.07)	20.52 (-21.08, 62.11)	21.52 (-17.93, 60.97)	22.46 (-17.84, 62.75)
LVOTI	-19.12 (-45.37, 7.12)	-33.51 (-68.39, 1.37)	<b>-42.24</b> <b>(-82.38, -2.10)</b>	<b>-41.67</b> <b>(-82.19, -1.13)</b>	<b>-51.98</b> <b>(-86.25, -17.71)</b>	<b>-54.02</b> <b>(-99.68, -8.36)</b>	-46.20 (-100.29, 7.90)	-46.55 (-101.34, 8.24)
LVMI	0.14 (-0.03, 0.31)	0.19 (0.01, 0.36)	0.15 (-0.03, 0.32)	0.15 (-0.03, 0.32)	-0.02 (-0.27, 0.23)	0.04 (-0.20, 0.29)	0.01 (-0.23, 0.24)	0.01 (-0.23, 0.25)
LAVI	0.01 (-0.41, 0.42)	0.10 (-0.33, 0.54)	0.14 (-0.28, 0.55)	0.12 (-0.30, 0.54)	-0.30 (-0.88, 0.28)	-0.12 (-0.70, 0.47)	-0.02 (-0.58, 0.53)	-0.02 (-0.58, 0.55)
AOI	-1.85 (-14.55, 10.86)	3.86 (-10.88, 18.60)	2.08 (-11.87, 16.03)	1.80 (-12.29, 15.89)	-4.21 (-21.92, 13.50)	8.84 (-10.72, 28.39)	6.34 (-12.08, 24.76)	6.47 (-12.21, 25.14)
LAI	-2.95 (-11.70, 5.79)	0.23 (-10.93, 11.38)	0.88 (-10.78, 12.53)	0.58 (-11.20, 12.37)	<b>-13.83</b> <b>(-25.42, -2.24)</b>	-7.02 (-21.75, 7.72)	-3.18 (-18.61, 12.26)	-3.09 (-18.67, 12.58)
LVEF	-0.07 (-0.47, 0.33)	0.10 (-0.36, 0.55)	0.08 (-0.35, 0.51)	0.09 (-0.35, 0.52)	0.002 (-0.56, 0.56)	0.40 (-0.19, 0.99)	0.44 (-0.12, 0.99)	0.43 (-0.13, 1.00)

CRAE: central retinal arteriolar equivalent; CRVE: central retinal venular equivalent; IVSSI: interventricular septum thickness at end systole index; IVSDI: interventricular septum thickness at end diastole index; LVIDDI: left ventricular internal diameter at end diastole index; LVIDSI: left ventricular internal diameter at end systole index; LVPWDI: left ventricular posterior wall at end diastole index; LVPWSI: left ventricular posterior wall at end systole index; LVOTI: left ventricular outflow tract index; LVMI: left ventricular mass index; LAVI: left atrial volume index; AOI: aortic diameter index; LAI: left atrium index; LVEF: left ventricular ejection fraction.

Beta and 95%CI are presented in the table, and values with statistically significance (p<0.05) are highlighted in boldface font.

Model 1 unadjusted model

Model 2 adjusted for sex and age

Model 3 adjusted for sex, age, MAP and BMI

Model 4 adjusted for sex, age, MAP, BMI and history of co-morbidity